

Application of Moment Analysis to Mass Transfer Kinetics of Reversed-Phase Liquid Chromatography: Part 1. Experimental Investigation of Measurement of the Third Central Moment

Hong Gao^{1,2,3}, Xiuhong Wu^{1,2}, and Bingchang Lin^{1,2,*}

¹School of Chemical Engineering, Dalian University of Technology, Dalian, Liaoning, 116024, China; ²Center of Separation Technology, University of Science and Technology Liaoning, Anshan, Liaoning, 114051, China; and ³Department of Physics, Anshan Normal University, Anshan, Liaoning, 114005, China

Abstract

The first three statistical moments of the eluted band profiles from reversed-phase liquid chromatographic columns were attempted to be measured and analyzed in this work. And in this first part, the effect of the experimental conditions on the measurement accuracy of the third central moment is investigated. The optimized experimental condition is determined under which the measurement accuracy of the third central moment is much improved. Further analysis of the measurement result of the third central moment (μ_3) shows that the linear correlation exists between $\mu_3 u_0^4$ and the flow velocity (u_0).

Introduction

Moment analysis of a chromatographic peak is an effective method of getting fundamental information about the chromatographic processes in a column and has been widely adopted by researchers. In practice, the first and second moments are frequently mentioned because they are easy to measure accurately. But as we know, only the first two moments cannot characterize a chromatographic peak completely, especially for the peak deviating from the Gaussian shape. Hence, in principle, the higher moments are needed to describe quantitatively the asymmetry of chromatographic peak, which is also related to the important chromatographic processes in the column.

In the 1960s, discussions about the higher moments of chromatographic peak have been reported by various groups. In 1965, Kubin (1) and Kucera (2) independently calculated the

moment equations. After then, many researchers (3) tried to apply the result of higher moments as a means for the research of chromatographic problems rather than using them only to characterize the shape of chromatographic peak. For example, Grushka et al. (4–6) used the first four moments, more specifically the skew and excess that are derived from these moments, to study the degree of overlapping of chromatographic peaks and to characterize the effect of the experimental conditions on the peak shape. H.A. Boniface et al. (7) analyzed the mass transfer parameters based on the first four moments. Higher moments were also used to describe the chromatographic performance of capillary column (8), to reflect the effect of adsorption/desorption kinetics for perfusive column (9), or to study the influence of the increased heating rate in programmed temperature gas chromatography (10). Some authors (11,12) also made efforts to improve the accuracy of the measurement of moments, but C. Vidal-Madjar et al. (13) pointed out the large measurement errors of the higher moments for gas chromatographic peak in the 1970s.

However, the consideration of the application of higher moments is still attractive for modern chromatography for the important information related to the basic physical-chemical column processes reflected by higher moments. In the modern study of the mass transfer kinetics of chromatography, the use of the higher moments has never been investigated. In this work, the statistic moments, especially the third central moment, of liquid chromatographic band profiles for retained and non-retained solutes are measured, respectively, and the results are analyzed. In this first part, the effect of the experimental conditions on the measurement accuracy of the third central moment is investigated to determine the suitable experimental condition under which the third central moment can be measured accurately.

*Author to whom correspondence should be addressed: e-mail bingchanglin@yahoo.com.

Statistical moments of the band profile

The n th central moment of an eluted band profile can be calculated according to the equations below:

$$\mu_n = \frac{\int_0^{\infty} C(t)(t - M_1)^n dt}{\int_0^{\infty} C(t) dt} \quad \text{Eq. 1}$$

$$M_1 = \frac{\int_0^{\infty} tC(t) dt}{\int_0^{\infty} C(t) dt} \quad \text{Eq. 2}$$

where M_1 is the average elution time of the solute and $C(t)$ is the concentration of solute detected at the end of the column at time (t).

The definitions seem simple, but actually the calculation of the moments of an experimental eluted band profile is not as simple as one expects at first glance. Guiochon and Lin (14,15) pointed out that the errors made in the moment calculation increased with the order of the moment because for higher moments, the contributions of the front and back parts of the band profile far from the center were important; and the signal-to-noise ratios (S/N) of these parts were generally low, which would result in the large errors of moments. This is why the moment with an order more than two was seldom used in practice.

Experimental

Chemicals

Uracil (99%, Alfa Aesar China Company, Tianjin, China) and phenylethane (99%, Alfa Aesar China Company) were used as the retained and non-retained solutes, respectively. Their statistical moments of band profiles were measured in this work.

A mixture of HPLC-grade methanol (Chinese National Medicines Corporation, Shanghai, China) and pure water, made in the Nano center of this university with a volume ratio of 80:20, was used as the mobile phase, and the solvent for uracil and phenylethane eluted from column 1. The mobile phase, which was also the solvent for phenylethane eluted from column 2, was analytical-grade isopropanol (Shenyang XinXi Reagent Factory, Shenyang, China).

Columns

Column 1 is a C_{18} column (250 mm \times 4.6 mm, Dikma Technologies, Beijing, China) with an average diameter of packing particles of 5 μ m. The total porosity (ϵ_t) was 0.66. The total length of the connecting stainless steel tubes from the sample injecting valve to the column head and from the column end to the detector was about 25 cm, and the inner diameter of the tube was 0.25 mm.

Column 2 is a stainless steel column (200 mm \times 10 mm) packed with C_{18} -bonded porous silica gel (Daiso Company, Osaka, Japan) in slurry-packing methods in our laboratory. The average particle diameter and the mean pore diameter of the

silica gel are 20 μ m and 140 angstroms, respectively. The total porosity (ϵ_t) of the column was 0.625. The total length of the connecting stainless steel tubes outside the column used for the moment measurement was about 44 cm with an inner diameter of 0.007 in (approximately 0.18 mm).

Apparatus

The LC-10ATvp solvent delivery module (Shimadzu, Kyoto, Japan) was used to deliver the mobile phase. The SPD-10Avp UV detector (Shimadzu) was adopted. And before measurement, the solvent delivery module and the UV detector were calibrated according to the validation procedures to make sure that they would perform normally during the measurements. The deviations of actual flow velocities of the mobile phase from the values set for the solvent delivery module were also checked, and they were no more than 0.02 mL/min. The fluctuation of the pressure of the overall system indicated by the solvent delivery module during measurements was 0.1–0.3 Mpa. The N2000 chromatographic workstation (Zhejiang University, Hangzhou, China) was connected to the UV detector to record and treat the signals from it. The 7725(i) manual sample injector (Rheodyne, Oak Harbor, WA) with a 20- μ L sample loop was used and with a sample injecting needle of 100 μ L. To avoid the possible effect of temperature, a water bath (Beijing YongGuangMing Medical Treatment Instrument Factory, Beijing, China) and a high-performance liquid chromatographic column heater/cooler (Shanghai Eastsen Analytical Instrument, Shanghai, China) were adopted. The temperature was set to be 25°C. And the connecting tubes were wrapped with foam for thermal insulation.

Procedure

The process of moment measurement is described as follows. In this work, the same process was performed for all the samples under different experimental conditions, which are listed in detail in Table I.

Prior to the experiment, the mobile phase was filtered (0.45- μ m pore diameter) and then placed in an ultrasonic vibration instrument for 15 min to get rid off the gas dissolved in it.

At various flow velocities of mobile phase, the pulses of sample

Table I. Experimental Conditions for the Samples

Condition	Sample	Mobile phase and solvent for the solute	Column*
A	Uracil solution (low conc.)	Methanol and pure water (80/20, v/v)	Column 1
B	Phenylethane (low conc.)	Methanol and pure water (80/20, v/v)	Column 1
C	Uracil solution (higher conc.)	methanol and pure water (80/20, v/v)	Column 1
D	Phenylethane solution (higher conc.)	methanol and pure water (80/20, v/v)	Column 1
E	Phenylethane	Isopropanol	Column 2

* Column 1: 250 mm \times 4.6 mm C_{18} column with the average diameter of packing particles of 5 μ m; column 2: 200 mm \times 10 mm C_{18} column with the average diameter of packing particles of 20 μ m.

solution were injected into the column, and the corresponding eluted band profiles were detected and recorded, the detecting wavelength used was 254 nm. For each flow velocity, the injection was repeated for five times for the purpose of calculating the average result of the moments as well as their standard deviations.

After the measurements of the band profiles eluted from column, the column was replaced by a connector without extra dead volume. And then similar experiments as outlined previously were performed in order to evaluate the effect of extra column.

Calculations of the Moments

For each sample eluted at every flow velocity, the zero to third moments of the eluted band profiles were calculated according to Eq. 1 and 2. Two kinds of moments were calculated. One is calculated based on the band profiles eluted from the columns in which the extra-column effect was involved; the other is calculated based on the eluted band profiles measured when the column being replaced by the connector. And then subtracted the latter from the former, the net values of the experimental moments of the samples in the column were obtained. Based on the repeatedly measured band profiles, the average values and the corresponding standard deviations of the moments were also obtained.

Determination of the start and stop points of the integral of

the statistical moments is especially important for the measurement of the higher moment. In this work, they were determined using the “baseline” and “find peak” tool of OriginPro 7.5 (OriginLab, Northampton, MA).

Results and Discussion

The measurement result of the third central moment at different flow velocities of mobile phase

The result of the net values of the third central moments in columns and the corresponding standard deviations at different flow velocities of mobile phase for different samples are shown in Figure 1. The detailed conditions of measurement for all the samples are described in Table I. To indicate clearly the decrease of the third central moment with flow velocity, the logarithmic scale is used for the y -axis in the figure. The lengths of the short vertical lines in the figures above and below data points equal to the absolute values of the standard deviations of the third central moments. For all the samples measured in this work, it is obvious that the value of the third central moment decreases with the flow velocity. The result is easy to understand; with the increase of flow velocity, the difference among the different flow patterns through the column lessens, and this leads to the decrease of the values of the second and third central moments.

The result of the standard deviations of the third central moments for all the samples is shown in Figure 2. To facilitate the comparison of the results obtained under different conditions, the relative standard deviation of the third central moments is adopted. Unlike the result of the third central moment shown in Figure 1, there is not a clear tendency of change of relative standard deviation with the increase of flow velocity shown in Figure 2. That is to say, the flow velocity does not have an obvious effect on the measurement error of the third central moment. What is clearly shown in Figure 2 is that the relative standard deviations of the third central moments of the samples of lower concentration [conditions (A) and (B)] are greater than those of the samples of higher concentration [conditions (C) and (D)]; furthermore, the best result of the third central moment is that measured under condition (E). The reason of this will be discussed later.

Effect of the S/N of eluted band profile on the measurement error of the third central moment

As previously mentioned, a baseline with much noise will affect the result of measurement of the third central moment. The carefully prepared mobile phase, the solvent delivery pump, and a detector with good performance can ensure us a relatively steady baseline. But the measurement result of the third central moments reflects the effect of the

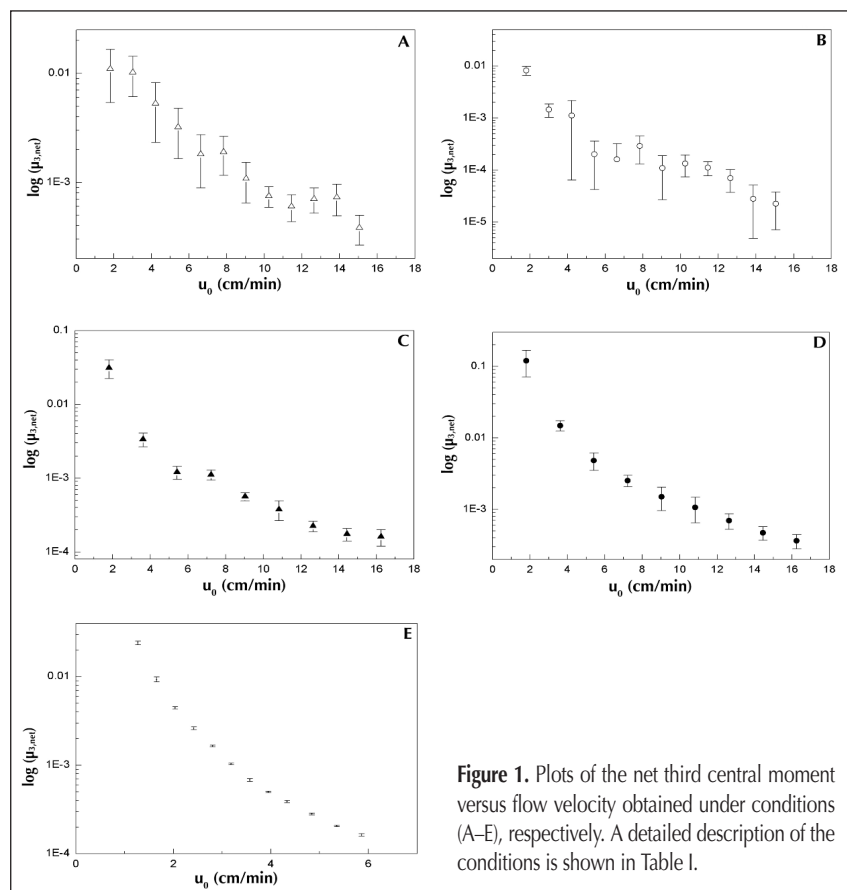


Figure 1. Plots of the net third central moment versus flow velocity obtained under conditions (A–E), respectively. A detailed description of the conditions is shown in Table I.

noise remarkable, especially when the S/N of the band profile is low. The S/N ratios of eluted band profiles obtained under different conditions are listed in Table II. The S/N ratio of a chromatographic peak obtained here equals the height of the peak divided by the standard deviation of the baseline noise (16). And because the peak height decreases with the flow velocity, the eluted band profiles of which the S/N ratios are investigated for different conditions should be those measured at similar flow velocities. The band profiles obtained under conditions (A)–(D) are measured at a flow velocity of 5.42 cm/min, and the band profile for condition (E) is measured at the flow velocity of 5.35 cm/min.

It is obvious in Table II that the S/N ratios of those band profiles are different. The S/N of band profile (E) is the highest, then band profiles (C) and (D) with finally the S/N ratios of band profiles (A) and (B) being the lowest. This is consistent with the result shown earlier of the relative standard deviation of the third central moment shown in Figure 2. So it is concluded that increasing the S/N ratio of the eluted band profile is an effective method to improve the measurement accuracy of the third central moment. However, it should be noted that the measurement error of the third central moment under condition (E) is much less than those under conditions (C) and (D), but the S/N ratio of the band profile obtained under condition (E) is not much larger than those obtained under conditions (C) and (D).

Table II. Signal-to-Noise Ratios of the Band Profiles Obtained Under Conditions (A–E)

	Signal-to-noise ratio
Band profile (A)*	1779
Band profile (B)*	2533
Band profile (C)*	40648
Band profile (D)*	41530
Band profile (E)*	47577

* The band profiles (A)–(D) in the table are measured at the flow velocity of 5.42 cm/min under conditions (A)–(D), respectively, and the band profile (E) is measured at the flow velocity of 5.35 cm/min under condition (E).

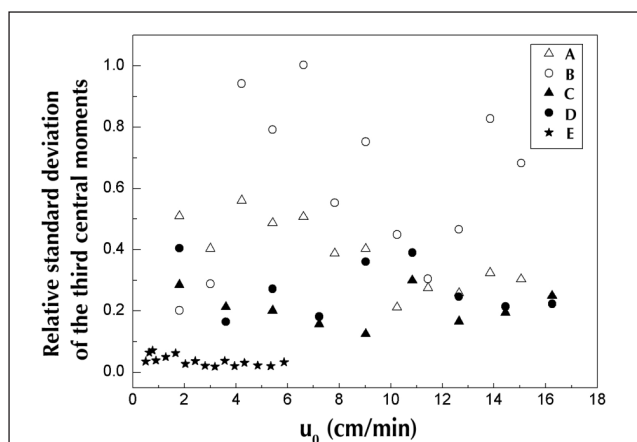


Figure 2. Plot of relative standard deviation of the third central moment versus flow velocity obtained under conditions (A–E), respectively. A detailed description of the conditions is shown in Table I.

This indicates that besides the higher S/N ratio, there is another factor that contributes to the low measurement error of the third central moment under condition (E).

Effect of the tailing of eluted band profile on the measurement of the third central moment

The effect of the tailing of eluted band profile on the measurement of the third central moment can be explained by the plots of the curves of $C(t)(t - M_1)^3 - t$, and they are shown in Figure 3. According to the definition of the moments, we know that the integral area under the curve of $C(t)(t - M_1)^3 - t$ divided by the value of $\int_0^\infty C(t)dt$ is the third central moment. So the analysis of the curve of $C(t)(t - M_1)^3 - t$ can facilitate the understanding of the measurement result of the third central moment.

It is easy to understand that if the eluted band profile is a Gaussian peak, then the corresponding curve of $C(t)(t - M_1)^3 - t$ is centrosymmetric. The areas surrounded by the curve above and below the baseline are same, so the third central moment of the band profile equals zero. Unlike what is mentioned for a Gaussian peak, different results can be found in Figure 3A–3D. This is due to the tailing of the eluted band profile and is discussed as follows.

It should be stated that although for each sample the curve of $C(t)(t - M_1)^3 - t$ at only one flow velocity is presented here, the characteristic of the curve is typical and exists for the band profiles eluted at other flow velocities.

Two subsections of the tail of the eluted band profile

It is well-known that two definitions are used to characterize the extent of the asymmetry of an eluted band profile, the asymmetry, and tailing factors, which reflects the difference between the front and back half-widths at 10% and 5% of the peak height, respectively. That is to say, the part of the tail of the band profile which is from 10% to 5% of the peak height is considered to be important to characterize the asymmetry of a peak. And in this work, this part of tail is named the tail of subsection I.

As for the measurement of the third central moment of an eluted band profile, it is not only the tail of subsection I that affects the measurement result. The tail of band profile that is located below 5% of the peak height still has important effect, which is named the tail of subsection II.

Table III. Asymmetry Factors of Eluted Profiles Obtained Under Conditions (A–E)

	Asymmetry factor
Band profile (A)*	1.78
Band profile (B)*	1.07
Band profile (C)*	1.51
Band profile (D)*	1.33
Band profile (E)*	1.06

* The profiles (A)–(E) in the table are those eluted profiles on which the calculated curves in Figure 3A–3E are based, respectively.

Effect of the tail of subsection I

This part of tail of band profile mainly affects the value of the measurement value of the third central moment, and this is explained below.

Just as shown in Figure 3A and 3C for uracil, after the positions indicated by the arrows, the curves continue rising, while for a Gaussian peak, from this position, the curve of $C(t)(t - M_1)^3 - t$ should begin to descend to the baseline. Such a difference is due to the slower descending speed of the tails of subsection I of uracil. That is to say, with the increase of time, for

the certain part of the peak tail the decrease of $C(t)$ cannot compensate the increase of $(t - M_1)^3$, so the value of $C(t)(t - M_1)^3$ continues rising. The large asymmetry factors of the eluted band profiles of uracil [conditions (A) and (C)] can account for the increase (Table III). Obviously, the unusual rising part of the curve of $C(t)(t - M_1)^3 - t$ can result in a larger value of the third central moment.

As for the situation of the eluted band profiles of phenylethane, whether measured under conditions (B), (D), or (E), the shape of the curve of $C(t)(t - M_1)^3 - t$ in Figure 3 is more like that of a Gaussian peak than those of the eluted band profiles of uracil. The result indicates their fast descending tail of subsection I, and it is a reasonable explanation for why the eluted band profiles of phenylethane have moderate asymmetry factors compared with those of uracil in Table III.

Effect of the tail of subsection II

We can also find that the very ends of the curves in Figure 3A and 3C turn to descend until they drop to the level of baseline. The result indicates that the band profiles of the uracil have a fast descending tail of subsection II. A slight fluctuant curve end in Figure 3A and a smooth curve end in Figure 3B can be observed. The effect of the noise is weakened by the fast descending of the tail of subsection II.

But for the curves in Figure 3B and Figure 3D, a descending end cannot be found, and the fluctuation of the curve end is remarkable. This means that with the increase of time, the decrease of $C(t)$ just compensates the increase of $(t - M_1)^3$, and hence the value of $C(t)(t - M_1)^3$ maintains a relatively constant level. Consequently, the effect of noise looks significant. Obviously, this is due to not having a fast enough descending tail of subsection II of the eluted band profiles obtained under conditions (B) and (D). And such a slowly descending end has a significant negative influence on the measurement of the third central moment, because the stop point of integral for the moment calculation is difficult to determine in this situation; and besides, a slight drift of the stop point of integral would result in a considerable deviation of the calculated value of the third central moment. So the slowly descending tail of subsection II of eluted band profile should be avoided during the measurement of the third central moment.

Improved experimental condition for the measurement of the third central moment

Based on the analysis done earlier, a consideration on how to improve the experimental condition for the measurement of the third central moment has been preliminary

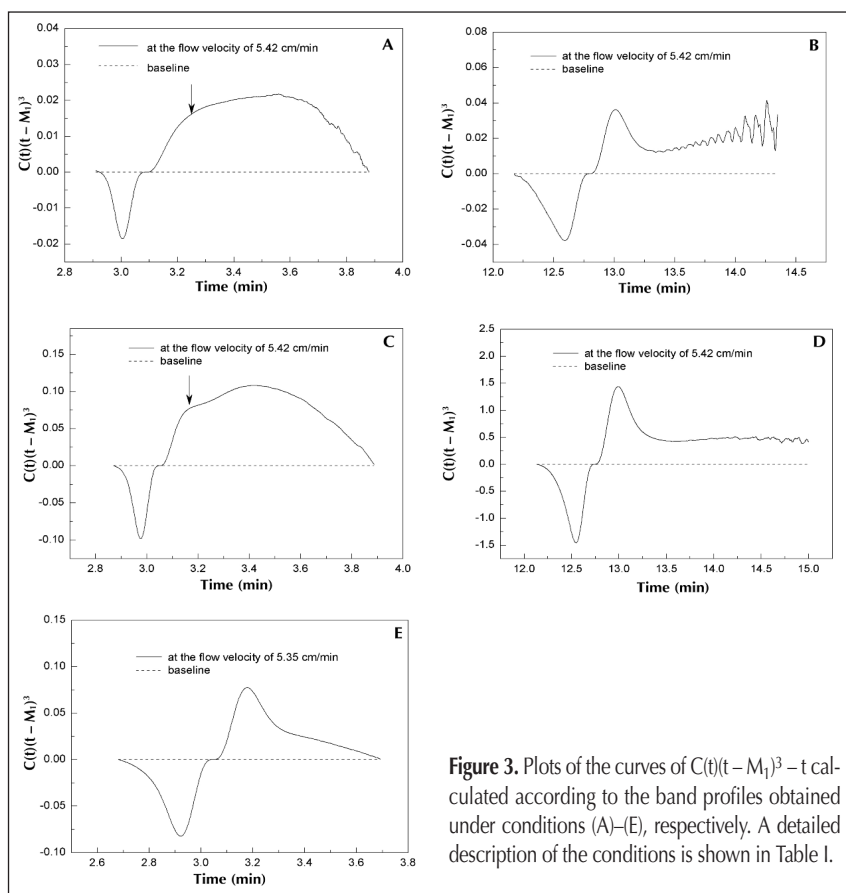


Figure 3. Plots of the curves of $C(t)(t - M_1)^3 - t$ calculated according to the band profiles obtained under conditions (A)–(E), respectively. A detailed description of the conditions is shown in Table I.

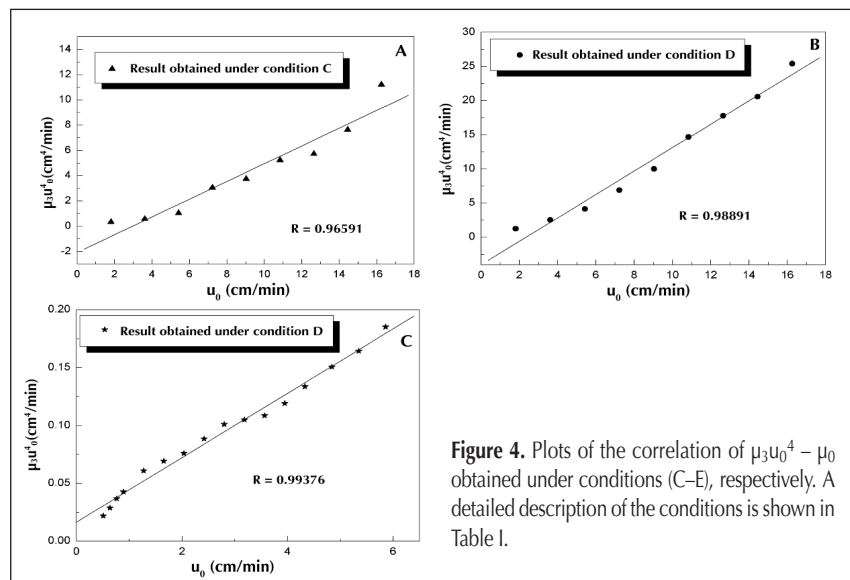


Figure 4. Plots of the correlation of $\mu_3 u_0^4 - \mu_0$ obtained under conditions (C)–(E), respectively. A detailed description of the conditions is shown in Table I.

narily formed. Firstly, the S/N ratio of the eluted band profile should be high. Secondly, the slowly descending tail of subsection II should be avoided. And the experimental condition (E) was then set up according to the consideration mentioned previously. The phenylethane was still used as the sample solute for its high purity. To reduce the tailing of eluted band profile especially for the tail of subsection II, a stronger eluent (i.e., isopropanol) was used. Considering the possible application of the measurement result of the third central moment in the analysis of the mass transfer kinetics of solute in column, the preparative column (column 2) was adopted, in which the packing particles has a average diameter of 20 μm to make the effect of intraparticle mass transfer remarkable.

The experimental result of the third central moment under condition (D) can be reflected in Figure 1E, Figure 2, Table II, and Figure 3E. The end of the curve in Figure 3E is ideal, which indicates an acceptable S/N ratio of the eluted band profile and that the slowly descending tail of subsection II was avoided successfully. All resulted in low standard deviations of the third central moment obtained under condition (E) and the regular distribution of the data points in Figure 1E which indicates the quantitative correlation between the third central moment and the flow velocity of mobile phase.

Further analysis about the result of the third central moment

The result of the third central moment obtained under condition (E) suggests us to make a further analysis of the correlation between the third central moment and the flow velocity. The result is shown in Figure 4C.

It is a plot of $\mu_3 u_0^4 - u_0$, and in the figure a clear linear correlation can be found. The value of the correlation coefficient shown in the figure also supports the result of linear regression. It is an interesting result, and it is credible because it is based on the measurement result of the third central moment with low standard deviations. And a similar analysis was also performed for the results of the third central moment obtained under conditions (C)–(D). The results obtained under conditions (A) and (B) are not considered here for their large standard deviations of the third central moments. The corresponding results are shown in Figure 4A–4B. Similar linear correlation of $\mu_3 u_0^4 - u_0$ can also be found.

In the analysis, the measurement results of the third central moment under three conditions are involved. Although relative large measurement errors of the third central moment are obtained under conditions (C) and (D), the linear correlation for $\mu_3 u_0^4 - u_0$ still can be found as that obtained under condition (E). The result shows that the linear correlation between $\mu_3 u_0^4$ and u_0 is not an occasional phenomenon that exists only for a single solute under a particular chromatographic condition. Is it helpful for the understanding of the mass transfer kinetics in column? Obviously, more work is needed to make the problem clear.

Conclusion

According to the results and discussions stated earlier, it is concluded that several conditions should be met to get the

measurement result of the third central moment of band profile with small error, and they are summarized as follows.

Apparatus with good performance, especially a steady solvent delivery system are needed. The purity of the sample solute should be high or at least the chromatographic resolution of the target compound and any impurity should be high enough. The high S/N ratio of the eluted band profile is necessary. The tailing of the eluted band profile should be limited, the long and flat end of the band profile, which is mentioned in this work as the slow descending tail of subsection II, should be avoided during the measurement.

Based on the analysis of the measurement results of the third central moment, the linear correlation of $\mu_3 u_0^4 - u_0$ is found. This is an interesting result, which should be further explored.

Acknowledgment

This work was supported by the fund of Group Project provided by Liaoning Education Department of China and the research foundation for Ph.D. Programs from Ministry of Education of China.

References

1. M. Kubin. Contribution to the theory of chromatography II: Influence of the diffusion outside and the adsorption within the sub-grains. *Collect. Czech. Chem. Commun.* **30**: 2900–2907 (1965).
2. E. Kucera. Contribution to the theory of chromatography: linear non-equilibrium elution chromatography. *J. Chromatogr.* **19**: 237–248 (1965).
3. E. Grushka, M.N. Myers, P.D. Schettler, and J.C. Giddings. Computer characterization of chromatographic peaks by plate height and higher central moments. *Anal. Chem.* **41**: 889–892 (1969).
4. E. Grushka, M.N. Myers, and J.C. Giddings. Moments analysis for the discernment of overlapping chromatographic peaks. *Anal. Chem.* **42**: 21–26 (1970).
5. E. Grushka. Characterization of exponentially modified Gaussian peaks in chromatography. *Anal. Chem.* **44**: 1733–1738 (1972).
6. E. Grushka. Chromatographic peak shapes: their origin and dependence on the experimental parameters. *J. Phys. Chem.* **76**: 2586–2593 (1972).
7. H.A. Boniface and D.M. Ruthven. The use of higher moments to extract transport data from chromatographic adsorption experiments. *Chem. Eng. Sci.* **40**: 1401–1409 (1985).
8. S.P. Cram, F.J. Yang, and A.C. Brown, III. Characterization of high performance glass capillary gas chromatography. *Chromatographia* **10**: 397–403 (1977).
9. A. Genga and K. C. Lohb. Effects of adsorption kinetics and surface heterogeneity on band spreading in perfusion chromatography: a network model analysis. *Chem. Eng. Sci.* **59**: 2447–2456 (2004).
10. B.J. McCoy. Moment theory of band spreading, skewness, and resolution in programmed temperature gas chromatography. *Sep. Sci. Technol.* **14**: 515–527 (1979).
11. S.N. Chesler and S.P. Cram. Effect of peak sensing and random noise on the precision and accuracy of statistical moment analyses from digital chromatographic data. *Anal. Chem.* **43**: 1922–1933 (1971).
12. S.N. Chesler and S.P. Cram. Digitization errors in the measurement of statistical moments of chromatographic peaks. *Anal. Chem.* **44**: 2240–2243 (1972).
13. C. Vidal-Madjar and G. Guiochon. Experimental characterization of elution profiles in gas chromatography using central statistical moments: study of the relationship between these moments and mass transfer kinetics in the column. *J. Chromatogr.* **142**: 61–86 (1977).
14. G. Guiochon and B.C. Lin. *Modeling for Preparative Chromatography*, Academic Press, Amsterdam, 2003, pp. 79.
15. G. Guiochon, A. Felinger, A.M. Katti, and D.G. Shirazi. *Fundamentals of Preparative and Nonlinear Chromatography*, 2nd ed., Academic Press, Amsterdam, 2006, pp. 312.
16. N. Dyson. *Chromatographic Integration Methods*, 2nd ed., R.M. Smith, Royal Society of Chemistry, Cambridge, England, 1998, pp. 54.